Journal of Engineering Mathematics, Vol. 7, No. 3, July 1973
Noordhoff International Publishing–Leyden
Printed in The Netherlands

Wave forces on a submerged vertical plate

M. STIASSNIE AND G. DAGAN

Hydraulics and Hydrodynamics Lab. and Dept. of Applied Mathematics, Technion-Israel Inst. of Technology, Haifa, Israel.

(Received May 26, 1972)

SUMMARY

A vertical plate of finite length and depth is attacked by gravity waves in water of finite depth. The forces and moments acting on the plate are computed by using the theory of linearized waves. The forces depend on three dimensionless parameters combining the draft, length, water depth and wave length and on the angle of attack. The problem is reduced to the solution of two infinite linear systems of equations. Numerical solutions are presented for different particular combinations of the parameter values. In most of the cases the standing wave approximation yields sufficiently accurate results.

1. Introduction

Gravity waves acting on ships and other floating bodies induce forces and moments which set them in motion. Computing the magnitude of the forces is a necessary step in order to determine the body motion as well the structure strength. In the usual engineering approach (Blagoveshchensky [2]) the forces are computed with neglect of scattering, and other additional simplifying assumptions are used. More advanced solutions are based on a slender-body approximation (Newman, [9]).

In the present work we compute the forces induced by a monochromatic wave approaching from infinity and impinging upon a rectangular vertical plate in water of finite depth. No approximations are involved excepting the usual linearization of the surface condition. Although the plate is a body of a highly schematized shape, the information obtained in this case is valuable for validating different approximate engineering approaches.

The present study is an extension of the similar, but much simpler, solutions obtained for cylinders of circular cross-section (Black, Mei and Bray [1] and Garrett [4]). The essence of the method, like in the simpler case, is the using of elliptical coordinates r, θ, z (Fig. 1) such that the

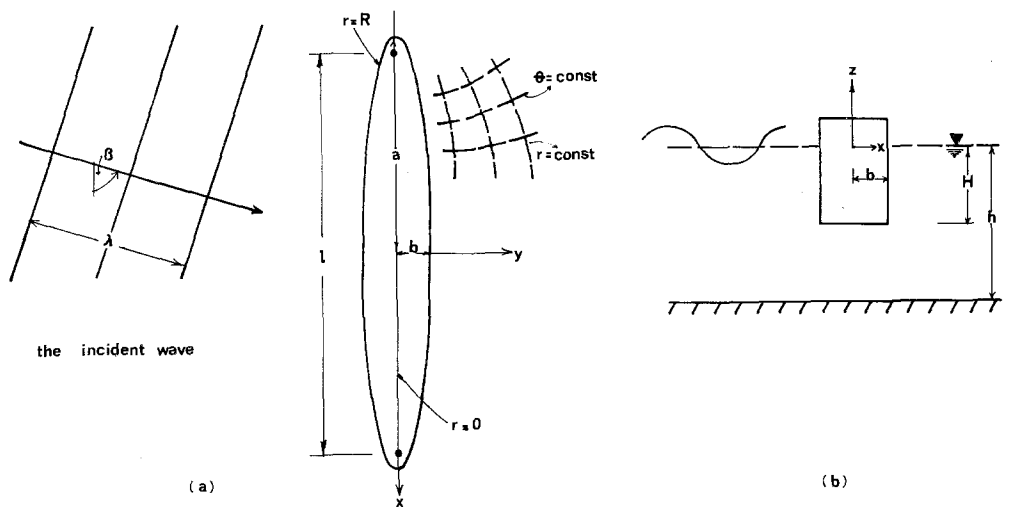

Figure 1. The elliptical cylinder: (a) view, (b) cross-section.

body plane contour becomes $r = R = \text{const}$. We start with the more general problem of a vertical elliptical cylinder, which degenerates into a plate as the ratio of lengths of the axis tends to zero.

2. Formulation of the mathematical problem

2.1. *General equations*

Elliptical coordinates (Fig. 1) are related to cartesian coordinates as follows

$$x = (l/2)\cosh r \cos\theta\,, \qquad (0 \leqq r < \infty\,,\quad 0 \leqq \theta < 2\pi) \tag{1a}$$

$$y = (l/2)\sinh r \sin\theta \tag{1b}$$

$$z = z\,. \tag{1c}$$

These are used in the sequel.

Under the assumption of linearized irrotational gravity waves, the velocity potential

$$\Phi(x, y, z, t) = \phi(x, y, z)e^{-i\omega t} \tag{2}$$

satisfies Laplace equation in the flow domain

$$\nabla^2\phi = 0 \tag{3}$$

and the free-surface equation

$$\phi_{,z} - \frac{\omega^2}{g}\phi = 0 \qquad (r > R,\ z = 0) \tag{4}$$

ω being the frequency.

The boundary condition at the bottom is

$$\phi_{,z} = 0 \qquad (z = -h) \tag{5}$$

while on the body surface we have

$$\phi_{,r} = 0 \qquad (r = R,\ -H < z < 0) \tag{6a}$$

$$\phi_{,z} = 0 \qquad (r < R,\ z = -H)\,. \tag{6b}$$

As usual the potential is represented as the sum

$$\phi = \phi^{\mathrm{I}} + \phi^{\mathrm{s}} \tag{7}$$

of the potentials of the incident and the scattered waves, respectively. The solution is rendered unique by imposing upon ϕ^{s} the radiation condition.

ϕ^{I} has the following expression

$$\phi^{\mathrm{I}} = \frac{ga}{\omega}\frac{f_1(z)}{f_1(0)}e^{ik_1\rho} \tag{8a}$$

where

$$\rho = x\cos\beta + y\sin\beta \tag{8b}$$

$$f_1(z) = 2^{\frac{1}{2}}\cosh[k_1(z+h)]/[h + (g/\omega^2)\sinh^2(k_1 h)]^{\frac{1}{2}} \tag{8c}$$

and a and k_1 are the amplitude and the wave number of the incident wave, respectively.

According to McLachlan [5] ϕ^{I} may be expressed in terms of elliptical coordinates as follows

$$\begin{aligned}\phi^{\mathrm{I}} = \frac{2ga}{\omega}\frac{f_1(z)}{f_1(0)}\sum_{m=0}^{\infty}\{&Ce_{2m}(r, q_1)\,ce_{2m}(\beta, q_1)\,ce_{2m}(\theta, q_1)/p_{2m}(q_1) + \\ &+ Se_{2m+2}(r, q_1)\,se_{2m+2}(\beta, q_1)\,se_{2m+2}(\theta, q_1)/s_{2m+2}(q_1) + \\ &+ i[Ce_{2m+1}(r, q_1)\,ce_{2m+1}(\beta, q_1)\,ce_{2m+1}(\theta, q_1)/p_{2m+1}(q_1) + \\ &+ Se_{2m+1}(r, q_1)\,se_{2m+1}(\beta, q_1)\,se_{2m+1}(\theta, q_1)/s_{2m+1}(q_1)]\}\end{aligned} \tag{9}$$

where $q_1=(\frac{1}{4}k_1 l)^2$, l is the body length (Fig. 1) and *Se*, *Ce*, *se* and *ce* are Mathieu functions (Appendix 1).

2.1. *Thin body expansion*

Rather than pursue the general problem of the elliptical cylinder, we consider the case of a thin body and expand ϕ as follows

$$\phi = \phi^{\mathrm{I}} + \phi_0^{\mathrm{s}} + \delta_1(R)\,\phi_1^{\mathrm{s}} + \ldots \tag{10}$$

where $R = o(1)$ and $\delta_1 = o(1)$.

Substituting ϕ from (10) into (3), (4), (5), and (6) and expanding for $r=R$, we find that ϕ_0^{s} satisfies the following equations

$$\nabla^2 \phi_0^{\mathrm{s}} = 0 \qquad (-h \leqq z \leqq 0) \tag{11a}$$

$$\phi_{0,z}^{\mathrm{s}} - (\omega^2/g)\phi_0^{\mathrm{s}} = 0 \qquad (r > 0,\ z = 0) \tag{11b}$$

$$\phi_{0,z}^{\mathrm{s}} = 0 \qquad (z = -h) \tag{11c}$$

$$\phi_{0,r}^{\mathrm{s}} = -\phi_{,r}^{\mathrm{I}} \qquad (r = 0,\ -H < z < 0) \tag{11d}$$

It is readily seen that by linearization the body boundary conditions are transferred from $r=R$ to $r=0$ and ϕ_0^{s} is the potential of the waves scattered by a vertical plate.

ϕ_1^{s} satisfies the same equations as ϕ_0^{s}, expecting (11d) which becomes

$$\phi_{1,r}^{\mathrm{s}} = -\phi^{\mathrm{I}}{}_{,rr} - \phi_{0,rr}^{\mathrm{s}} \qquad (r = 0,\ -H < z < 0) \tag{12}$$

while $\delta_1(R) = R$.

3. The solution of ϕ_0^{s}

Following the usual procedure of separation of variables ϕ_0^{s} is expressed as

$$\phi_0^{\mathrm{s}} = Z(z)\,\Theta(\theta)\,R(r) \tag{13}$$

Eqs. (11a), (13) yield for Z, Θ, R (Moon and Spencer, [6])

$$Z'' - (16\alpha/l^2)Z = 0 \tag{14a}$$

$$\Theta'' + (\delta_m - 2\alpha\cos 2\theta)\Theta = 0 \tag{14b}$$

$$R'' - (\delta_m - 2\alpha\cosh 2r)R = 0 \tag{14c}$$

where δ_m are eigenvalues (Appendix 1). The general solution of φ_0^{s}, satisfying (11a, b, c) and the radiation condition, is given by

$$\begin{aligned}\phi_0^{\mathrm{s}} = \sum_{m=0}^{\infty} \{ & b_{m1}^* f_1(z)\, Me_m^{(1)}(r, q_1)\, ce_m(\theta, q_1) + \\ & + \sum_{n=2}^{\infty} b_{mn}^* f_n(z)\, Fek_m(r, -q_n)\, ce_m(\theta, -q_n)\} + \\ & + \sum_{m=1}^{\infty} \{ b_{m1} f_1(z)\, Ne_m^{(1)}(r, q_1)\, se_m(\theta, q_1) + \\ & + \sum_{n=2} b_{mn} f_n(z)\, Gek_m(r, -q_n)\, se_m(\theta, -q_n)\}\end{aligned} \tag{15}$$

where b_{mn}^*, b_{mn} are unknown coefficients and $Me^{(1)}$, $Ne^{(1)}$, *Fek Gek*, *ce se*, are Mathieu functions (Appendix 1). The function $f_1(z)$ is given by (8c), while $f_n(z)$ $(n=2, 3, \ldots)$ are normalized eigenfunctions

$$f_n(z) = 2^{\frac{1}{2}} \cos[(4q_n^{\frac{1}{2}}/l)(z+h)] / [h - (g/\omega^2)\sin^2(4q_n^{\frac{1}{2}} h/l)]^{\frac{1}{2}} \tag{16}$$

with q_n $(n=1, 2, 3, \ldots)$ satisfying the following transcendental equations

$$(4q_1^{\frac{1}{2}}/l)\,\mathrm{th}\,[4q_1^{\frac{1}{2}}/l)h] = \omega^2/g \tag{17a}$$

$$(4q_n^{\frac{1}{2}}/l)\,\mathrm{tg}\,[4q_n^{\frac{1}{2}}/l)h] = -\omega^2/g\,, \qquad (n=2, 3, \ldots) \tag{17b}$$

The unknown coefficients in (15) have to be determined with the aid of (11d) and from the requirement of continuity beneath the plate

$$\phi_0^s(r, \theta, z) = \phi_0^s(r, -\theta, z) \qquad (r=0, -h<z<-H) \tag{18a}$$

$$\phi_{0,r}^s(r, \theta, z) = -\phi_{0,r}^s(r, -\theta, z)\,. \qquad (r=0, -h<z<-H) \tag{18b}$$

Since most of the wave energy is concentrated in the vicinity of the free surface, it is convenient to represent ϕ_0^s as

$$\phi_0^s = \bar{\phi} + \tilde{\phi} \tag{19}$$

where $\bar{\phi}$ is the potential of the waves scattered by a plate penetrating through the whole water depth. Hence $\bar{\phi}$ satisfies the following body condition.

$$\bar{\phi}_{,r} = -\phi_{,r}^I\,. \qquad (r=0, -h<z<0) \tag{20}$$

A similar problem has been solved by Morse and Rubinstein [7] in the case of scattering of electromagnetic waves. Using their solution it is easy to ascertain that $\bar{\phi}$ has the following expression

$$\bar{\phi} = f_1(z) \sum_{m=1}^{\infty} \bar{b}_{m1} Ne_m^{(1)}(r, q_1)\, se_m(\theta, q_1) \tag{21}$$

where $\bar{b}_{m1}$ are known coefficients given in Appendix 1. The potential $\tilde{\phi}$ satisfies at $r=0$ the following boundary conditions [see (20)]:

$$\tilde{\phi}_{,r}(0, \theta, z) = -\tilde{\phi}_{,r}(0, -\theta, z) \qquad (-h<z<-H) \tag{22a}$$

$$\tilde{\phi}_{,r}(0, \theta, z) = 0 \qquad (-H<z<0) \tag{22b}$$

$$\tilde{\phi}(0, \theta, z) - \tilde{\phi}(0, -\theta, z) = \bar{\phi}(0, -\theta, z) - \bar{\phi}(0, \theta, z)\,. \qquad (-h<z<-H) \tag{22c}$$

$\tilde{\phi}$ may be regarded as the potential of the flow generated by a wavemaker beneath the plate which cancels the velocity potential discontinuity associated with $\bar{\phi}$. The velocity distribution at the "wavemaker" is selected as an unknown function represented by the following double series

$$\tilde{\phi}_{,r} = \sum_{t=1}^{\infty} \sum_{s=1}^{\infty} U_{ts} F_s(z) \sin t\theta \qquad (r=0, -h<z<-H) \tag{23a}$$

$$\tilde{\phi}_{,r} = 0\,. \qquad (r=0, -H<z<0) \tag{23b}$$

By retaining in (23a) only odd functions of θ, Eq. (22a) is satisfied identically. The orthonormal set $F_n(z)$ is given by

$$F_1(z) = (h-H)^{-\frac{1}{2}} \tag{24a}$$

$$F_n(z) = [2/(h-H)]^{\frac{1}{2}} \cos[(n-1)\pi(h+z)/(h-H)]\,, \qquad (n=2, 3, \ldots) \tag{24b}$$

so that (11c) is satisfied. The constants U_{ts} are unknown coefficients to be determined with the aid of (22c). The potential $\tilde{\phi}$ may be represented again in the whole flow domain by a series similar to that of (15), retaining only odd functions of θ, as follows:

$$\tilde{\phi} = \sum_{m=1}^{\infty} \{\tilde{b}_{m1} f_1(z)\, Ne_m^{(1)}(r, q_1)\, se_m(\theta, q_1) + \sum_{n=2}^{\infty} \tilde{b}_{mn} f_n(z)\, Gek_m(r, -q_n)\, se_m(\theta, -q_n)\}\,. \tag{25}$$

The following relationships between $\tilde{b}_{mn}$ in (25) and the "wavemaker" coefficients U_{ts} in (23a)

are found by differentiating $\tilde{\phi}$ (25), setting $r=0$ and identifying with $\tilde{\phi}_{,r}$ in (23a,b):

$$\tilde{b}_{(2m+1)1} = \frac{1}{Ne^{(1)}_{2m+1}(0, q_1)} \sum_{t=0}^{\infty} \sum_{s=1}^{\infty} U_{(2t+1)s} P_{1s} B^{2m+1}_{2t+1}(q_1) \tag{26a}$$

$$\tilde{b}_{(2m+2)1} = \frac{1}{Ne^{(1)}_{2m+2}(0, q_1)} \sum_{t=0}^{\infty} \sum_{s=1}^{\infty} U_{(2t+2)s} P_{1s} B^{2m+2}_{2t+2}(q_1) \tag{26b}$$

$$\tilde{b}_{(2m+1)n} = \frac{1}{Gek'_{2m+1}(0, -q_n)} \sum_{t=0}^{\infty} \sum_{s=1}^{\infty} U_{(2t+1)s} P_{ns} (-1)^{m+t} A^{2m+1}_{2t+1}(q_n) \tag{26c}$$

$$\tilde{b}_{(2m+2)n} = \frac{1}{Gek'_{2m+2}(0, -q_n)} \sum_{t=0}^{\infty} \sum_{s=1}^{\infty} U_{(2t+2)s} P_{ns} (-1)^{m+t} B^{2m+2}_{2t+2}(q_n) \tag{26d}$$

where P_{ns} $(n=1, 2, \ldots; s=1, 2, \ldots)$, $B^m_t(q)$ $A^m_t(q)$ are known coefficients defined in Appendix 1.

The only unknown coefficients U_{ts} satisfy the equations derived from (22c) by using the eigenfunctions of $\tilde{\phi}_{,r}$ from (23a)

$$\int_0^{2\pi} d\theta \sin \tau\theta \int_{-h}^{-H} dz F_\psi(z) \{[\bar{\phi}(0, \theta, z) + \tilde{\phi}(0, \theta, z)] - [\bar{\phi}(0, -\theta, z) + \tilde{\phi}(0, -\theta, z)]\} = 0$$
$$(\tau = 1, 2, \ldots; \psi = 1, 2, \ldots) \tag{27}$$

Substituting $\bar{\phi}$ from (21) and $\tilde{\phi}$ from (25) in (27) and using (26), we finally obtain after some algebraic manipulations the following infinite systems of linear equations for U_{ts}:

$$\sum_{t=0}^{\infty} \sum_{s=1}^{\infty} U_{(2t+1)s} D^{(2\tau+1)\psi}_{(2t+1)s} = \bar{D}^{(2\tau+1)\psi}, \qquad (\tau = 0, 1, \ldots; \psi = 1, 2, \ldots) \tag{28a}$$

$$\sum_{t=0}^{\infty} \sum_{s=1}^{\infty} U_{(2t+2)s} D^{(2\tau+2)\psi}_{(2t+2)s} = \bar{D}^{(2\tau+2)\psi}, \qquad (\tau = 0, 1, \ldots; \psi = 1, 2, \ldots) \tag{28b}$$

where the coefficients $D^{\tau\psi}_{ts}$ and $\bar{D}^{\tau\psi}$, which are expressed in terms of known quantities, are given in Appendix 1.

Concluding, the original problem for ϕ^s_0 has been reduced to the solution of the infinite systems of Eqs. (28).

Once these systems are solved, U_{ts} are substituted in (26) to obtain $\tilde{\phi}$ which added to $\bar{\phi}$ (21) yields ϕ^s_0. The systems (28) have been solved numerically by taking only a finite number of terms. Unfortunately the convergence of the partial solution towards the exact one could not be proved rigorously because of the complex structure of the coefficients of (28). Instead the number of equations has been gradually increased until the values of U_{ts}, as well as those of the forces, became practically constant. Since this constancy was reached quite rapidly by using a relatively small number of terms, it was concluded that the system is well behaved, at least in the range of values of parameters considered here. This conclusion has been strengthened by the good agreement between the present computations and other known solutions for some particular cases (see Section 6).

The numerical procedure and the practical convergence test are discussed in some detail in Appendix 2.

It is worthwhile to point out that the splitting of ϕ^s_0 in the two components $\bar{\phi}$ and $\tilde{\phi}$ and the representation of $\tilde{\phi}$ in terms of the wavemakers coefficients U_{ts} improve significantly the convergence of the solution of the resulting infinite systems.

4. Forces acting on the elliptical cylinder

The linearized pressure P acting on the surface of the body is given by

$$P = -\gamma z + \frac{i\omega\gamma}{g} e^{-i\omega t} [\phi^I(0, \theta, z) + \phi^s_0(0, \theta, z) + O(R)]$$

where γ is the specific weight of the fluid.

The expressions for the various forces and moments are found by integrating the pressure on the body surface

$$F_x' = \frac{l}{2}\sinh R\int_{-H}^{0}\int_{0}^{2\pi} dz\,d\theta\,P(R,\theta,z)\cos\theta =$$

$$= \frac{i\omega\gamma l\,e^{-i\omega t}}{2g}\left\{R\int_{-H}^{0}\int_{0}^{2\pi} dz\,d\theta\,\phi^{I}(0,\theta,z)\cos\theta + O(R^2)\right\}, \tag{29a}$$

$$F_y' = \frac{l}{2}\cosh R\int_{-H}^{0}\int_{0}^{2\pi} dz\,d\theta\,P(R,\theta,z)\sin\theta =$$

$$= \frac{i\omega\gamma l\,e^{-i\omega t}}{2g}\left\{\int_{-H}^{0}\int_{0}^{2\pi} dz\,d\theta\,\phi_0^{s}(0,\theta,z)\sin\theta + O(R)\right\}, \tag{29b}$$

$$F_z' = \frac{l^2}{2}\int_{0}^{R}\int_{0}^{2\pi} dr\,d\theta\,P(r,\theta,-H)\sin^2\theta = \frac{\pi\gamma H l^2\sinh 2R}{8} +$$

$$+ \frac{i\omega\gamma l^2\,e^{-i\omega t}}{4g}\left\{R\int_{0}^{2\pi} d\theta\,\phi^{I}(0,\theta,-H)\sin^2\theta + O(R^2)\right\}, \tag{29c}$$

$$M_x' = \frac{l}{2}\cosh R\int_{-H}^{0}\int_{0}^{2\pi} dz\,d\theta\,P(R,\theta,z)z\sin\theta + \frac{l^2}{4}\int_{0}^{R}\int_{0}^{2\pi} dr\,d\theta\,P(r,\theta,-H)y\sin^2\theta =$$

$$= \frac{2\omega\gamma\,e^{-i\omega t}}{2g}\left\{-\int_{-H}^{0}\int_{0}^{2\pi} dz\,d\theta\,\phi_0^{s}(0,\theta,z)z\sin\theta + O(R)\right\}, \tag{29d}$$

$$M_y' = \frac{l}{2}\sinh R\int_{-H}^{0}\int_{0}^{2\pi} dz\,d\theta\,P(R,\theta,z)z\cos\theta - \frac{l^2}{4}\int_{0}^{R}\int_{0}^{2\pi} dr\,d\theta\,P(r,\theta,-H)x\sin^2\theta =$$

$$= \frac{i\omega\gamma l\,e^{-i\omega t}}{2g}\left\{R\left[\int_{-H}^{0}\int_{0}^{2\pi} dz\,d\theta\,\phi^{I}(0,\theta,z)z\cos\theta - \right.\right.$$

$$\left.\left. - \frac{l^2}{4}\int_{0}^{2\pi} d\theta\,\phi^{I}(0,\theta,-H)\cos\theta\sin^2\theta\right] + O(R^2)\right\}, \tag{29e}$$

$$M_z' = \frac{l^2}{8}\int_{-H}^{0}\int_{0}^{2\pi} dz\,d\theta\,P(R,\theta,z)\sin 2\theta =$$

$$= \frac{i\omega\gamma\,e^{-i\omega t}}{2g}\left\{\int_{-H}^{0}\int_{0}^{2\pi} dz\,d\theta\,\phi_0^{s}(0,\theta,z)\sin 2\theta + O(R)\right\}. \tag{29f}$$

In deriving (29a)–(29f) advantage was taken of the fact that $\phi^{I}(0,\theta,z)$ in (9) and $\phi_0^{s}(0,\theta,z)$ in (15) are even and odd functions of θ, respectively.

Eqs. (29a, 29c, 29e) show that the first approximations of F_x', F_z', M_y' of order R result from the integration of the pressure induced by the incident wave solely over the body surface. The simple computation of these components is not pursued here.

The other three forces, the lateral ones, F_y', M_x', M_z' in (29b, 29d, 29f) depend in the first order only on the scattered wave and are determined by the pressure distribution on the equivalent plate.

Writing down the complete solution of ϕ_0^{s} as

$$\phi_0^{s} = \bar{\phi} + \tilde{\phi} = \sum_{m=1}^{\infty}\left\{b_{m1}f_1(z)Ne_m^{(1)}(r,q_1)se_m(\theta.q_1) + \right.$$

$$\left. + \sum_{n=2}^{\infty} b_{mn}f_n(z)Gek_m(r,-q_n)se_m(\theta,-q_1)\right\} \tag{30}$$

where $b_{mn}=\bar{b}_{mn}+\tilde{b}_{mn}$ are known constants, we obtain by integrating in (29)

$$|F_y| = \frac{|F_y'|}{\gamma a l H} = \frac{\pi\omega}{2agH}\sum_{m=1,3,5}^{\infty}\left\{b_{m1}L_1 Ne_m^{(1)}(0,q_1)B_1^m(q_1)+ \right.$$
$$\left. + \sum_{n=2,3\ldots}^{\infty} b_{mn}L_n Gek_m(0,-q_n)(-1)^{(m-1)/2}A_1^m(q_n)\right\}, \quad (31a)$$

$$|M_x| = \frac{|M_x'|}{\gamma a l H^2} = \frac{\pi\omega}{2agH^2}\sum_{m=1,3,5}^{\infty}\left\{b_{m1}K_1 Ne_m^{(1)}(0,q_1)B_1^m(q_1)+ \right.$$
$$\left. + \sum_{n=2,3\ldots}^{\infty} b_{mn}K_n Gek_m(0,-q_n)(-1)^{(m-1)/2}A_1^m(q_n)\right\}, \quad (31b)$$

$$|M_z| = \frac{|M_z|}{\gamma\alpha l^2 H} = \frac{\pi\omega}{8agH}\sum_{m=2,4,6}^{\infty}\left\{b_{m1}L_1 Ne_m^{(1)}(0,q_1)B_2^m(q_1)+ \right.$$
$$\left. + \sum_{n=2,3\ldots}^{\infty} b_{mn}L_n Gek_m(0,q_n)(-1)^{(m-2)/2}B_2^m(q_n)\right\}, \quad (31c)$$

where

$$L_n=\int_{-H}^{0} f_n(z)dz \quad \text{and} \quad K_n=\int_{-H}^{0} zf_n(z)dz\,.$$

Again, the values of the forces depend ultimately on the coefficients U_{ts} in (28).

5. The small wave length limit (geometrical optics)

It turns out (Section 6) that an useful approximation for the forces is obtained at the limit of small wave length λ as compared to H and l. At this limit the incident wave is just reflected by the plate. Hence ϕ has the following expressions

$$\phi=0 \quad \text{if} \quad y\cot\beta-l/2<x<y\cot\beta+l/2\,, \qquad y>0\,; \quad (32a)$$

$$\phi = \frac{ag}{\omega}\frac{f_1(z)}{f_1(0)}e^{-i\omega t}\left[e^{ik_1(x\cos\beta+y\sin\beta)}+e^{ik_1(x\cos\beta-y\sin\beta)}\right] \quad (32b)$$

$$\text{if } -y\cot\beta-l/2<x<y\cot\beta+l/2\,, \qquad y<0\,;$$

$$\phi=\phi^{\mathrm{I}}=\frac{ag}{\omega}\frac{f_1(z)}{f_1(0)}e^{-i\omega t}e^{ik_1(x\cos\beta+y\sin\beta)} \text{ elsewhere}\,. \quad (32c)$$

ϕ of (32b) represents a standing wave in front of the plate. The forces acting on the plate, originating from the standing waves at the upstream face, are found by using (29) as follows:

$$|F_y| = \frac{2|\sin[(l/\lambda)\pi\cos\beta]|}{(l/\lambda)\pi\cos\beta}\cdot\frac{\sinh[(h/\lambda)2\pi]-\sinh[(h/\lambda-H/\lambda)2\pi]}{(H/\lambda)\,2\pi\cosh[(h/\lambda)2\pi]}, \quad (33a)$$

$$|M_x| = \frac{2|\sin[\pi\cos\beta(l/\lambda)]|}{(l/\lambda)\pi\cos\beta}\cdot\left\{\frac{(2\pi h/\lambda)\sinh(2\pi h/\lambda)-\cosh(2\pi h/\lambda)}{(2\pi H/\lambda)^2\cosh(2\pi h/\lambda)}\right.$$
$$-\frac{2\pi(h/\lambda-H/\lambda)\sinh[2\pi(h/\lambda-H/\lambda)]-\cosh[2\pi(h/\lambda-H/\lambda)]}{(2\pi H/\lambda)^2\cosh(2\pi h/\lambda)}$$
$$\left.-\frac{(2\pi h/\lambda)\sinh[2\pi(h/\lambda-H/\lambda)]-(2\pi h/\lambda)\sinh(2\pi h/\lambda)}{(2\pi H/\lambda)^2\cosh(2\pi h/\lambda)}\right\}, \quad (33b)$$

$$|M_z| = \frac{|(l/\lambda)\pi\cos\beta\cos[(l/\lambda)\pi\cos\beta]-\sin[(l/\lambda)\pi\cos\beta]|}{[(l/\lambda)\pi\cos\beta]^2}$$
$$\cdot\frac{\sinh[(h/\lambda)2\pi]-\sinh[(h/\lambda)-H/\lambda)2\pi]}{(H/\lambda)2\pi\cosh[(h/\lambda)2\pi]}. \quad (33c)$$

6. Discussion of numerical results

6.1. *General*

The lateral forces and moments (31a,b,c) acting on the body depend on four dimensionless parameters: the draft/length ratio H/l, the depth/length ratio h/l, the incident wave length/length ratio λ/l and the angle of attack β.

Because of the multitude of parameters and the tedious numerical computations, the forces have been computed only for a few particular combinations of the parameter values. Generally, three of the parameters have been kept constant, and the remaining one assigned various values.

The different stages of the numerical computations which ultimately yielded the values of U_{ts} in (28) and of the forces, as well as a sample of the numerical convergence, are given in detail in Appendix 2.

It is worthwhile mentioning that the forces (31) have been made dimensionless with respect to hydrostatical forces acting on a body of finite beam. The magnitude of the forces reflects, therefore, the role played by the dynamical wave effect.

6.2. *The influence of the wave length*

Three parameters have been kept fixed: $H/l=0.1$, $h/l=0.2$ and $\beta=90°$. The draft/wavelength ratio H/λ has been taken equal to 0.1, 0.2 and 0.5 (i.e., $h/\lambda=0.2, 0.4, 1$ and $l/\lambda=1, 2, 5$ respectively). These are, therefore, typical cases of waves in water of finite depth up to deep water and of waves of moderate to short length as compared with l. The ratio $H/h=0.5$ is not particularly significant, since the wave energy is concentrated mostly in the upper zone of the flow domain.

The computed values of $|F_y|$ and $|M_x|$ in (31a,b) are represented in Fig. 2. On the same figure we have represented the forces computed by Black, Mei and Bray [1] in the case of an infinite strip ($l\to\infty$), i.e. of two-dimensional flow. To adopt the latter values in the case of a finite l is somehow tantamount to using a "strip" theory. In addition, the forces based on the standing wave approximation (33 a,b) have been also represented in Fig. 2.

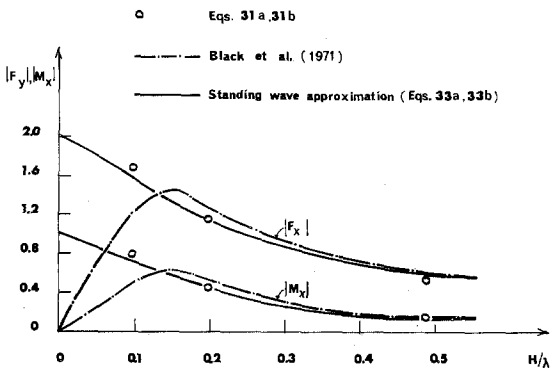

Figure 2. The influence of H/λ on the lateral wave forces $|F_y|$ and $|M_x|$ for $h/l=0.2$, $H/l=0.1$ and $\beta=90°$.

In most of the range investigated here, say for $H/\lambda>0.15$, the solution is in excellent agreement with the two-dimensional solution. Consequently, the influence of the edge refraction is small. Moreover, the simple short wave length approximation is also very close to the present solution, even in the range $0.1<H/\lambda<0.15$. The range $H/\lambda<0.1$ has not been investigated because of the numerical difficulties. This range, however, can be handled easier with the aid of other approximate approaches, like those of slender body (Newman, [9]) or shallow water (Tuck and Taylor [11]).

At the limit $H/\lambda\to0$ with G/h and H/l kept fixed (i.e. $h/\lambda\to0$ and $l/\lambda\to0$) the flow degenerates into a streaming motion beneath a rigid wall. This case has been treated by Newman [10]. The forces vanish for $H/\lambda=0$, but the short wave approximation is then no more valid.

6.3. *The influence of the angle of attack*

The influence of the variation of β upon the three lateral forces and moments has been studied for two sets of values of the other parameters: $\lambda/l=0.5$, $h/l=0.2$, $H/h=0.5$ (Fig. 3) and $\lambda/l=1$, $h/l=0.2$, $H/h=0.5$ (Fig. 4). The moment M_z has been computed for easiness with $H/h=1$. In

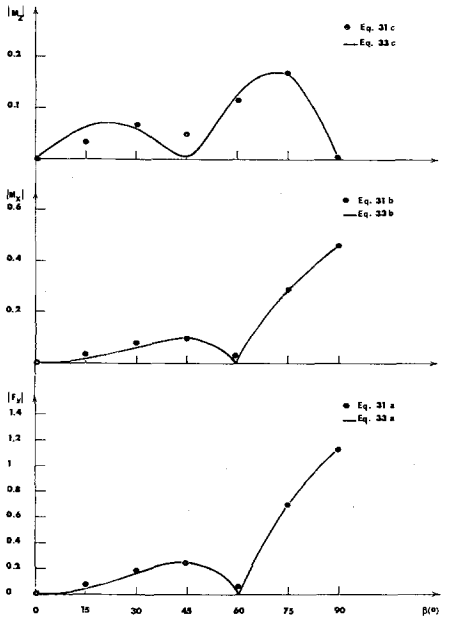

Figure 3. The influence of β on the lateral wave forces $|F_y|$ and $|M_x|$ for $h/l=0.2$, $H/l=0.1$ and $\lambda/l=0.5$ and on $|M_z|$ for $h/l=0.2$, $H/l=0.2$ and $\lambda/l=0.5$.

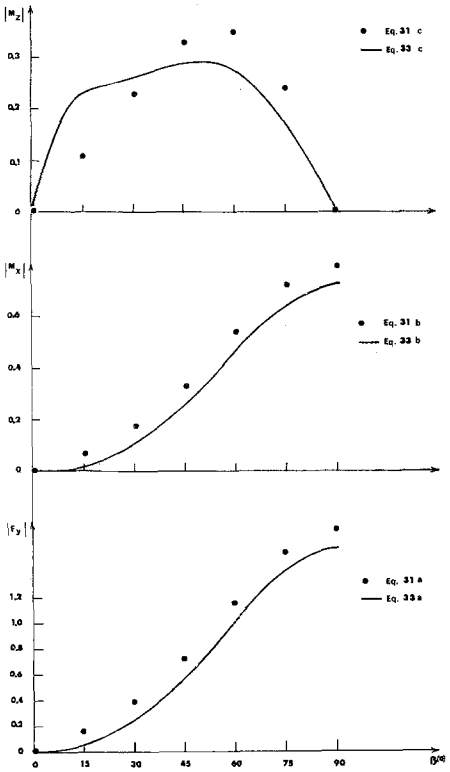

Figure 4. The influence of β on the lateral wave forces $|F_y|$ and $|M_x|$ for $h/l=0.2$, $H/l=0.1$ and $\lambda/l=1$, and on $|M_z|$ for $h/l=0.2$, $H/l=0.2$ and $\lambda/l=1$.

both Figs. 3 and 4 the forces computed with the aid of the small-wave-length approximation are also represented.

In the first case of the smaller λ (Fig. 3) the agreement between the present solution and the standing wave approximation is very good for $|F_y|$ and $|M_x|$. As for $|M_z|$ the difference is larger because of the relatively large contribution of the pressure at the edges (29f).

The cancellation of $|F_y|$ and $|M_z|$ for $\beta=60°$ is just a result of the projection of the crests and troughs of the standing waves upon the body surface.

In the case of the larger wave length (Fig. 4) the agreement between the present and the standing wave solution is still fair.

In all cases $|F_y|$ and $|M_x|$ drop quite rapidly as β decreases from its maximum value of 90°.

6.4. *The influence of the draft*

We have taken $\lambda/l=0.5$, $\lambda/l=0.2$ and $\beta=90°$ and let H/h vary from $H/h=1$ (no bottom clearance) to $H/h=0.25$ (Fig. 5). Again the solution is in excellent agreement with the standing-

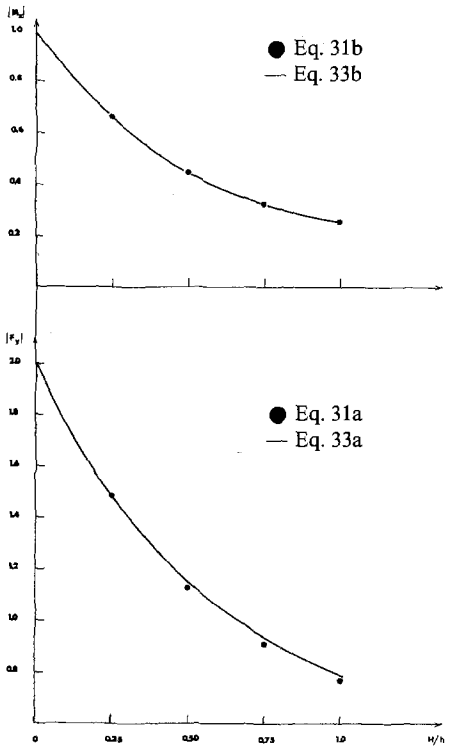

Figure 5. The influence of H/h on the lateral wave forces $|F_y|$ and $|M_x|$ for $h/l=0.2$, $\lambda/l=0.5$ and $\beta=90°$.

wave solution. The dimensionless forces increase as H/h becomes small apparently because of the uneven distribution of the wave energy with depth.

It is worthwhile to mention here that at the limit $H/h=0$, with λ/h and λ/l kept fixed, $|F_y|$ and $|M_x|$ are different from zero, although the numerical values obtained from the small-wave-length approximation are probably not correct. Even a body of vanishing draft causes wave scattering and F_y' and M_y' are proportional to H and H^2, respectively for small H/h.

Again, the solution for smaller H/h than considered here can be approached by slender body approximations.

6.5. *The influence of the water depth*

We have also checked the influence of the change of h/l upon the forces in the range $h/l=0.2$ to

1.0 while keeping $\lambda/l=0.5$, $H/l=0.1$ and $\beta=90°$. The values of the forces have been found to vary as follows: $|F_x|=1.13$ to 0.96 and $|M_x|=0.46$ to 0.39, respectively. The forces change only slightly, because $\lambda/h=2.5$ to 0.5 corresponds to waves in almost deep water.

7. Conclusions

The lateral wave forces acting on a thin elliptical body have been computed by using the theory of wave scattering without any additional approximation concerning the draft or the wave length. The results are, therefore, particularly valuable in those ranges of the dimensionless parameters of the problem in which other known approximations (slender body, shallow water) are not sufficiently accurate.

The method used in the present work is too elaborate to be of a practical value for solving any given particular case. Fortunately, the results show that for elongated bodies (say $l/H>10$) and for not too large wave lengths (say $\lambda/l<1$, $\lambda/H<10$) the forces may be obtained quite accurately from the simple approximation of standing waves.

In the case of large wave lengths other approximate methods can be used in order to obtain the forces in a simpler way than the present method.

The wave forces are generally of the same order of magnitude as the hydrostatical forces and they should be taken into account in any realistic computation of the body motion.

Appendix 1: Definition and computation of different coefficients and functions.

1. The parameter α in Mathieu equations (14) takes the values $\alpha=q_1$, $-q_n$ $(n=2, 3, \ldots)$ with
$$q_1=(\pi l/2\lambda)^2 \tag{A.1}$$
and q_2 q_3, ... the solutions of the transcendental equation (17b), which has been solved numerically.
2. The eigenvalues $\delta_m(q_n)$ of Mathieu equation (14) have been partially taken from N.B.S. [8] tables and computed for large q_n with the aid of the asymptotic formula of McLachlan [5].
3. The different Mathieu functions (9), (15) have been computed by using the series given in McLachlan [5], e.g.
$$se_{2m+1}(\beta, q_1)=\sum_{r=0}^{\infty} B_{2r+1}^{2m+1}(q_1)\sin[(2r+1)\beta] \tag{A.2}$$
$$Se_{2m+1}(R, q_1)=\frac{s_{2m+1}}{B_1^{2m+1}}\sum_{r=0}^{\infty}(-)^r B_{2r+1}^{2m+1}[J_r(v_1)J_{r+1}(v_2)-J_{r+1}(v_1)J_r(v_2)] \tag{A.3}$$
where $v_1=q_1^{\frac{1}{2}}\exp(-R)$; $v_2=q_1^{\frac{1}{2}}\exp(R)$.
The Fourier coefficients of the type $B_{2r+1}^{2m+1}(q_1)$ in (31) have been computed by using the recursive formula given by Blanch [3].
4. The coefficients $\bar{b}$, $\bar{b}^*$ in (21) have been computed according to the following equations
$$\bar{b}_{m1}^*=\bar{b}_{mn}^*=\bar{b}_{mn}=0 \qquad (m=0, 1, 2, \ldots;\ n=2, 3, \ldots) \tag{A.4a}$$
$$\bar{b}_{(2m+1)1}=-\frac{2agi}{\omega f_1(0)}Se'_{2m+1}(0, q_1)\,se_{2m+1}(\beta, q_1)/s_{2m+1}(q_1)Ne_{2m+1}^{(1)}(0, q_1), \qquad (m=0, 1, \ldots) \tag{A.4b}$$
$$\bar{b}_{(2m+1)1}=-\frac{2ag}{\omega f_1(0)}Se'_{2m+2}(0, q_1)\,se_{2m+2}(\beta, q_1)/s_{2m+2}(q_1)Ne_{2m+2}^{(1)\prime}(0, q_1), \qquad (m=0, 1, \ldots \tag{A.4c}$$
the coefficients $s_m(q_n)$ being defined in McLachlan [5].
5. The coefficients of the linear systems (28) have the following expressions.

$$D^{(2\tau+1)\psi}_{(2t+1)s} = \sum_{m=0}^{\infty} \Big\{ P_{1s}P_{1\psi}\, B^{2m+1}_{2t+1}(q_1)B^{2m+1}_{2\tau+1}(q_1)Ne^{(1)}_{2m+1}(0,q_1)/Ne^{(1)'}_{2m+1}(0,q_1) + \\ + \sum_{n=2}^{\infty} P_{ns}P_{n\psi}(-1)^{\tau+t}A^{2m+1}_{2t+1}(q_n)A^{2m+1}_{2\tau+1}(q_n)Gek_{2m+1}(0,-q_n)/Gek'_{2m+1}(0,-q_n)\Big\}, \tag{A.5a}$$

$$\bar{D}^{(2\tau+1)\psi} = \sum_{m=0}^{\infty} 2iP_{1\psi}B^{2m+1}_{2\tau+1}(q_1)\,se_{2m+1}(\beta,q_1)\cdot \\ \cdot [Ne^{(1)}_{2m+1}(0,q_1)/Ne^{(1)'}_{2m+1}(0,q_1)][Se'_{2m+1}(0,q_1)/s_{2m+1}(q_1)], \tag{A.5b}$$

$$D^{(2\tau+2)\psi}_{(2t+2)s} = \sum_{m=0}^{\infty} \Big\{ P_{1s}P_{1\psi}\, B^{2m+2}_{2t+2}(q_1)B^{2m+2}_{2\tau+2}(q_1)Ne^{(1)}_{2m+2}(0,q_1)/Ne^{(1)'}_{2m+2}(0,q_1) + \\ + \sum_{n=2}^{\infty} P_{ns}P_{n\psi}(-1)^{\tau+t}B^{2m+2}_{2t+2}(q_n)B^{2m+2}_{2\tau+2}(q_n)\cdot \\ \cdot Gek_{2m+2}(0,-q_n)/Gek'_{2m+2}(0,-q_n)\Big\}, \tag{A.5c}$$

$$\bar{D}^{(2\tau+2)\psi} = \sum_{m=0}^{\infty} 2P_{1\psi}B^{2m+2}_{2\tau+2}(q_1)\,se_{2m+2}(\beta,q_1)\cdot \\ \cdot [Ne^{(1)}_{2m+2}(0,q_1)/Ne^{(1)'}_{2m+2}(0,q_1)]\cdot[Se'_{2m+2}(0,q_1)/s_{2m+2}(q_1)] \tag{A.5d}$$

In (A.5a)–(A.5d) P_{ns} are defined as

$$P_{n1} = \int_{-H}^{0} f_n(z)F_1(z)dz = \frac{[2/(h-H)]^{\frac{1}{2}}\sin k_n(h-H)}{[-h-(g/\omega^2)k_nh]^{\frac{1}{2}}k_n} \qquad (n=2,3,\ldots) \tag{A.6a}$$

$$P_{ns} = \int_{-H}^{0} f_n(z)F_s(z)dz = \frac{2(-1)^{n-1}}{(h-H)^{\frac{1}{2}}}\,\frac{k_n\sin[k_n(h-H)]}{[h-(g/\omega^2)\sin^2k_nh]^{\frac{1}{2}}(k_n^2-K_m^2)} \qquad (n,s=2,3,5\ldots) \tag{A.6b}$$

where $K_m=(m-1)\pi/(h-H)$ and $k_n=4q_n^{\frac{1}{2}}/l$. For $n=1$ k_n should be replaced by ik_1.

Appendix 2: The solution of the infinite linear system (28).

The system (28) has been truncated to a finite number of equations by taking a finite number of terms in the "wavemaker" equation (23a). The far terms in (23a) represent high-frequency components of the wavemaker motion and their influence is presumably negligible.

To check empirically the convergence of the solution of (28), the number of terms has been gradually increased until the solution became practically constant. As an example we give in

TABLE 1.

An example of coefficient convergence
for $H/h=0.5$, $\beta=90°$, $h/l=0.2$ and $\lambda/l=0.5$

L_1	L_2	$Re\{U_{11}\}$	$Im\{U_{11}\}$	GC	$\lvert F_y\rvert$
10	2	1.093	−0.796	1.2196	1.1285
10	3	1.082	−0.783	1.2150	1.1304
10	4	1.076	−0.774	1,2111	1.1314
10	5	1.073	−0.770	1.2092	1.1318
4	5	1.067	−0.751	1.1801	1.1340
6	5	1.072	−0.768	1.2071	1.1320
8	5	1.072	−0.770	1.2092	1.1318
10	5	1.073	−0.770	1.2092	1.1318

L_1, L_2 are the number of functions of θ and z, respectively, taken in (23a).

Table 1 the changes of $|F_y|$ and U_{11} from (31) and (28) as the number of terms in (28) is increased. In the same table the global coefficient of energy scattering

$$GC = \frac{\omega^2}{2la^2g^2} \int_S |\phi_0^s|^2 dS \tag{A.7}$$

is represented (S is an ellipse at $t \to \infty$).

The apparently good convergence of both $|F_y|$ and GC, which represent near and far field quantities respectively, suggests that (28) is well behaved and may be approximated by a not too large finite system. Generally, the number of terms necessary in order to obtain almost constancy and monotoneity of the numerical results did not exceed 50.

REFERENCES

[1] J. L. Black, C. C. Mei and M. C. Bray, Radiation and scattering of water waves by rigid bodies, *J. Fluid Mech.*, 46, (1971) 151–164.
[2] S. N. Blagoveshchensky, *Theory of ship motion*, Dover Publications, New York (1962).
[3] G. Blanch, On the computation of Mathieu functions, *J. Math. Phys.*, 25 (1946) 1–20.
[4] C. J. R. Garrett, Waves forces on a circular dock, *J. Fluid Mech.*, 46 (1971) 129–139.
[5] N. W. McLachlan, *Theory and application of Mathieu functions*, Dover Publications (1964).
[6] P. Moor and D. E. Spencer, *Field theory handbook*, Springer–Verlag (1961).
[7] P. M. Morse and P. J. Rubenstein, The diffraction of waves by ribbons and slits, *Physical Review*, 54 (1938) 895–898.
[8] National Bureau of Standards, *Tables relating to Mathieu functions*, App. Math. Series, 59 (1967).
[9] J. N. Newman, Applications of slender-body theory in ship hydrodynamics, *Ann. Rev. Fluid Mech.*, 2 (1970) 67–94.
[10] J. N. Newman, Lateral motion of a slender body between two parallel walls. *J. Fluid Mech.*, 39, (1969) 97–115.
[11] E. O. Tuck and P. J. Taylor, Shallow water problems in ship hydrodynamics, *Proc. 8th. Symp. on Naval Hydrodynamics*, (in press), (1970).